Analysis of the Vignale-Kohn current functional in the calculation of the optical spectra of semiconductors

Berger, J. A.; de Boeij, P. L.; van Leeuwen, R.

Published in:
Physical Review. B: Condensed Matter and Materials Physics

DOI:
10.1103/PhysRevB.75.035116

Publication date:
2007

Analysis of the Vignale-Kohn current functional in the calculation of the optical spectra of semiconductors

J. A. Berger, P. L. de Boeij, and R. van Leeuwen
Theoretical Chemistry, Materials Science Centre, Rijksuniversiteit Groningen, Nijenborgh 4, 9747AG Groningen, The Netherlands
(Received 14 July 2006; revised manuscript received 31 October 2006; published 16 January 2007)

In this work, we investigate the Vignale-Kohn current functional when applied to the calculation of optical spectra of semiconductors. We discuss our results for silicon. We found qualitatively similar results for other semiconductors. These results show that there are serious limitations to the general applicability of the Vignale-Kohn functional. We show that the constraints on the degree of nonuniformity of the ground-state density and on the degree of the spatial variation of the external potential under which the Vignale-Kohn functional was derived are almost all violated. We argue that the Vignale-Kohn functional is not suited to use in the calculation of optical spectra of semiconductors since the functional was derived for a weakly inhomogeneous electron gas in the region above the particle-hole continuum, whereas the systems we study are strongly inhomogeneous and the absorption spectrum is closely related to the particle-hole continuum.

DOI: 10.1103/PhysRevB.75.035116 PACS number(s): 71.45.Gm, 31.15.Ew, 78.20.−e, 78.66.Db

I. INTRODUCTION

Time-dependent density functional theory (TDDFT) developed by Runge and Gross[1] makes it possible to describe the dynamic properties of interacting many-particle systems in an exact manner.[1–4] Dhara and Ghosh[5] and Ghosh and Dhara[6] showed that the Runge-Gross theorem could be extended to systems that are subjected to general time-dependent electromagnetic fields (see also Ref. 7). The method has proven to be an accurate tool in the study of electronic response properties.[3,8,9] In this paper, we study infinite systems for which we use time-dependent current-density-functional theory (TDCDFT).[7,10–12] In this approach, the electron density of TDDFT is substituted by the electron current density as the fundamental quantity. There are mainly three reasons to use TDCDFT instead of ordinary TDDFT. The first reason is related to the use of periodic boundary conditions, which provide an efficient way to describe infinite systems but that artificially remove the effects of density changes at the surface.[13] For example, when a system is perturbed by an electric field there will be a macroscopic response of the system and a current will be flowing through the interior with a nonzero average given by $\mathbf{j}(t)=(1/\mathcal{V})\int_{\mathcal{V}}\mathbf{j}(\mathbf{r},t)d\mathbf{r}$, which is the spatial average of the current density $\mathbf{j}(\mathbf{r},t)$ over an arbitrary volume $\mathcal{V}$. This macroscopic current is directly related through the continuity equation to a density change at the outer surface of the system but does not correspond to a density change in the bulk of the system. The density change at the surface of the system leads to a macroscopic screening field in the bulk of the system. When using periodic boundary conditions, this phenomenon cannot be described with a functional of the bulk density alone,[13] but it can be described by a functional of the current density in the bulk. Some of these difficulties can be circumvented by use of an expression that relates the density-density response function to the trace of the current-current response function.[9,14,15] However, for anisotropic materials, this relation only provides enough information to extract the trace of the dielectric tensor and not its individual components. Second, in TDDFT, only the response caused by longitudinal vector potentials can be accounted for since only purely longitudinal vector potentials can be gauge transformed to scalar potentials. The scalar potential is the natural conjugate variable of the density in the meaning of a Legendre transform.[4] However, when we consider transverse vector potentials, the natural Legendre conjugate is the current density.[16] Third, to describe nonlocal exchange-correlation effects in large systems,[15,17,18] it can be more convenient and more efficient to use a local functional of the current density instead of a nonlocal functional of the density.[19–21] Within TDDFT, one would need an exchange-correlation functional that is completely nonlocal to be able to take into account the charges that are induced at the surface of the system caused by the external field and that produce a counteracting field.[13,22] Instead, by applying a local functional of the current density, we can still take into account nonlocal effects that are induced in the system by an external field.

TDDFT has mainly been used within the adiabatic local density approximation (ALDA) in which the exchange-correlation scalar potential $v_{xc}(\mathbf{r},t)$ is just a local functional of the density. In this work, we investigate a method that goes beyond the ALDA in which we employ an exchange-correlation vector potential, $\mathbf{A}_{xc}(\mathbf{r},t)$, the longitudinal part of which can be related to $v_{xc}(\mathbf{r},t)$ by a gauge transformation. We approximate the exchange-correlation vector potential as a local functional of the current density using the expression derived by Vignale and Kohn.[11,12] By studying a weakly inhomogeneous electron gas, they found a dynamical exchange-correlation vector potential as a functional of the current density that is nonlocal in time but still local in space. It was later shown by Vignale *et al.*[23] that the exchange-correlation vector potential obtained by Vignale and Kohn[11,12] could be recast in terms of a viscoelastic stress tensor, making the formalism physically more transparent. The Vignale-Kohn (VK) functional was derived under the constraints $k,q\ll k_F,\omega/v_F$, where k is the length of the wave vector of the external perturbation, q is the length of the wave vector of the inhomogeneity of the ground-state density, and k_F and v_F are the local Fermi wave vector and velocity, respectively. The constraint $q\ll k_F,\omega/v_F$ means

that, formally, the application of the VK functional is only justified if the ground-state density is slowly varying, and the constraint $k \ll k_F, \omega/v_F$ means we are formally allowed to use the VK functional if the induced current density is slowly varying. Furthermore, the constraint $k \ll \omega/v_F$ implies the region above the particle-hole continuum of the homogeneous electron gas.

The VK functional was first applied by Ullrich and Vignale to study the line widths of collective modes in two dimensional quantum strips and the line widths of intersubband plasmons in quantum wells.[24–27] These phenomena occur in the region above the particle-hole regime. They obtained a quantitative agreement with the experimentally observed linewidths of the intersubband plasmons. We then applied the VK functional in an approximated fashion as a polarization functional and observed that the dielectric functions of several semiconductors were much improved.[28] However, to obtain results in good agreement with experiment, an empirical prefactor had to be used. Later van Faassen *et al.*[19,20] showed that the inclusion of the VK functional in TDDFT calculations yields greatly improved polarizabilities for π-conjugated polymers, obtaining results that are comparable to MP2 values. These results were indications that the VK formalism is a very promising one, even when it is applied to describe phenomena related to the particle-hole regime in systems of which the ground-state density nor the induced current density is slowly varying. However, more recent results show that there are serious limitations to the general applicability of the VK functional. It was observed by van Faassen and de Boeij that the excitation energies of $n \rightarrow \pi^*$ transitions in π-conjugated polymers and a benchmark set of molecules are greatly overestimated.[21,29] A similar overestimation was found by Ullrich and Burke for the excitation energies of $s \rightarrow p$ transitions in atoms.[30] A recent review of the Vignale-Kohn functional applied to atoms and molecules can be found in Ref. 31. Finally, in a recent article,[32] we showed that the peak that appears in the optical spectra of one- and three-dimensional polyacetylene, which is a π-conjugated polymer, shows a large shift to higher frequency with respect to the peak that appears in the spectra obtained within the ALDA. Furthermore, the height of this peak is largely reduced. However, to obtain agreement with optical spectra from BSE calculations on three-dimensional polyacetylene[33,34] the height of the peak should increase and its width should decrease with respect to the peak in the ALDA spectrum. These results raise the question whether or not it is justified to apply the VK functional to inhomogeneous systems in the calculation of phenomena related to the particle-hole regime, such as optical spectra and excitation energies. In this work, we will try to answer this question. To do so we will study some limiting behavior of the VK functional and evaluate the VK functional when applied in the calculation of the optical spectra of silicon. We also performed calculations on several other semiconductors and insulators, namely, GaAs, GaP, and diamond, and found qualitatively similar results. Silicon was mainly chosen because it is a material for which the optical spectra obtained within the ALDA clearly show deficiencies, most notably the absence of the first peak in the absorption spectrum, and therefore, it is a good test system for methods that, such as VK, go beyond the ALDA.

The outline of this paper is as follows. In Sec. II, we give an overview of the theory we use; it consists of an account of linear response theory within TDCDFT, an introduction to the VK functional, an analysis of the limiting behavior of the response kernels of the electron gas which enter the VK functional, and a short summary of the parametrizations that are available for these kernels. The computational details are discussed in Sec. III. We present and discuss our results obtained for the optical spectra of silicon in Sec. IV. Finally, we draw conclusions from our findings in Sec. V.

II. THEORY

A. TDCDFT linear response equations

A frequency-dependent electric field $\mathbf{E}_{\text{ext}}(\omega)$ applied to a solid will induce a macroscopic polarization $\mathbf{P}_{\text{mac}}(\omega)$, which can be obtained from the induced current density $\delta\mathbf{j}(\mathbf{r},\omega)$ by [we use atomic units ($e=\hbar=m=1$) throughout this paper]

$$\mathbf{P}_{\text{mac}}(\omega) = \frac{-i}{\omega V}\int_V \delta\mathbf{j}(\mathbf{r},\omega)d\mathbf{r}, \tag{1}$$

where V is the volume of a unit cell. Within the linear response regime, the macroscopic polarization will be proportional to the macroscopic field $\mathbf{E}_{\text{mac}}(\omega)$, i.e., the applied field plus the average induced field within the solid. The constant of proportionality is the electric susceptibity $\chi_e(\omega)$,

$$\mathbf{P}_{\text{mac}}(\omega) = \chi_e(\omega)\cdot\mathbf{E}_{\text{mac}}(\omega). \tag{2}$$

Unlike $\mathbf{P}_{\text{mac}}(\omega)$ and $\mathbf{E}_{\text{mac}}(\omega)$, the susceptibility $\chi_e(\omega)$ is independent of the size and shape and is therefore a bulk property of the system. The induced current density can, in principle, be calculated from the true current-current response function $\chi_{\mathbf{jj}}(\mathbf{r},\mathbf{r}',\omega)$ of the system according to

$$\delta\mathbf{j}(\mathbf{r},\omega) = \frac{-i}{\omega}\int \chi_{\mathbf{jj}}(\mathbf{r},\mathbf{r}',\omega)d\mathbf{r}'\cdot\mathbf{E}_{\text{mac}}(\omega). \tag{3}$$

From Eqs. (1)–(3), it follows that

$$\chi_e(\omega) = \frac{-1}{\omega^2}\frac{1}{V}\int_V d\mathbf{r}\int d\mathbf{r}'\chi_{\mathbf{jj}}(\mathbf{r},\mathbf{r}',\omega). \tag{4}$$

The direct evaluation of the current-current response function is, however, unpractical. In our method, we therefore adopt a Kohn-Sham formulation in which the response to an external electric field of an interacting system is calculated as the response of an auxiliary noninteracting system to an effective field described by the set of Kohn-Sham potentials $\{\delta v_s(\mathbf{r},\omega), \delta\mathbf{A}_s(\mathbf{r},\omega)\}$. We choose the field $\mathbf{E}_{\text{mac}}(\omega)$ to be given and its relation to $\delta\mathbf{A}_{\text{mac}}(\omega)$ is given by $\delta\mathbf{A}_{\text{mac}}(\omega) = \mathbf{E}_{\text{mac}}(\omega)/i\omega$. We leave the relation between $\mathbf{E}_{\text{mac}}(\omega)$ and $\mathbf{E}_{\text{ext}}(\omega)$ unspecified because this depends on the sample size and shape and requires knowledge of $\chi_e(\omega)$. The set of Kohn-Sham potentials has the property that it produces the exact induced current density in the Kohn-Sham system. From the exact induced current density, we can calculate the exact induced density $\delta\rho(\mathbf{r},\omega)$ according to the continuity equation,

$$\nabla \cdot \delta\mathbf{j}(\mathbf{r},\omega) = i\omega\delta\rho(\mathbf{r},\omega). \tag{5}$$

The effective field is a functional of the induced current density and has to be solved in a self-consistent manner. To first order, we have the following expressions within the Kohn-Sham scheme for the induced density:

$$\delta\rho(\mathbf{r},\omega) = \int \{\chi_{s,\rho\mathbf{j}_p}(\mathbf{r},\mathbf{r}',\omega)\cdot\delta\mathbf{A}_s(\mathbf{r}',\omega) + \chi_{s,\rho\rho}(\mathbf{r},\mathbf{r}',\omega)\delta v_s(\mathbf{r}',\omega)\}d\mathbf{r}' \tag{6}$$

and the induced current density,

$$\delta\mathbf{j}(\mathbf{r},\omega) = \int \{[\chi_{s,\mathbf{j}_p\mathbf{j}_p}(\mathbf{r},\mathbf{r}',\omega) + \rho_0(\mathbf{r})\delta(\mathbf{r}-\mathbf{r}')]\cdot\delta\mathbf{A}_s(\mathbf{r}',\omega) + \chi_{s,\mathbf{j}_p\rho}(\mathbf{r},\mathbf{r}',\omega)\delta v_s(\mathbf{r}',\omega)\}d\mathbf{r}', \tag{7}$$

where $\rho_0(\mathbf{r})$ is the ground-state density. Here, the $\chi_{s,ab}$ are the Kohn-Sham response kernels, which are properties of the ground state. They are given by

$$\chi_{s,ab}(\mathbf{r},\mathbf{r}',\omega) = \lim_{\eta\to 0^+}\sum_{n,n'}(f_n - f_{n'}) \times \frac{[\phi_n^*(\mathbf{r})\tilde{a}\phi_{n'}(\mathbf{r})][\phi_{n'}^*(\mathbf{r}')\tilde{b}\phi_n(\mathbf{r}')]}{\omega-(\epsilon_{n'}-\epsilon_n)+i\eta}, \tag{8}$$

in which $\tilde{a}$ and $\tilde{b}$ can be either $\tilde{\rho}=1$ or $\tilde{\mathbf{j}}_p=-i(\nabla-\nabla^\dagger)/2$, where the dagger on the ∇ operator indicates that the operator acts on terms to the left of it. We use a tilde instead of a caret in the auxiliary operators $\tilde{\rho}$ and $\tilde{\mathbf{j}}_p$ in order to differentiate them from the density operator and paramagnetic current-density operator. In Eq. (8), f_n and ϵ_n are the occupation numbers and the eigenvalues, respectively, of the Kohn-Sham orbitals $\phi_n(\mathbf{r})$ of the unperturbed system. The positive infinitesimal η in Eq. (8) ensures the causality of the response function. In principle, the scalar potential could have been gauge transformed into a vector potential[26,27] and $\delta\rho(\mathbf{r},\omega)$ could have been expressed in terms of $\delta\mathbf{j}(\mathbf{r},\omega)$ by means of the continuity equation [Eq. (5)]. For the implementation, it is, however, convenient to include both the induced density and the scalar potential in our formalism. If we neglect the small Landau diamagnetic part, which is only important in the evaluation of magnetic properties, we can use the approximate conductivity sum rule[14]

$$[\chi_{s,\mathbf{j}_p\mathbf{j}_p}(\mathbf{r},\mathbf{r}',0)]_{ij} + \rho_0(\mathbf{r})\delta_{ij}\delta(\mathbf{r}-\mathbf{r}') = 0. \tag{9}$$

This sum rule can be used to relate the diamagnetic contribution to the induced current density $\delta\mathbf{j}_d=-\rho_0(\mathbf{r})\delta\mathbf{A}_s(\mathbf{r},\omega)$ to the static Kohn-Sham response function $\chi_{s,\mathbf{j}_p\mathbf{j}_p}(\mathbf{r},\mathbf{r}',0)$. With this approximation, we now obtain for the induced current density

$$\delta\mathbf{j}(\mathbf{r},\omega) = \int \{[\chi_{s,\mathbf{j}_p\mathbf{j}_p}(\mathbf{r},\mathbf{r}',\omega) - \chi_{s,\mathbf{j}_p\mathbf{j}_p}(\mathbf{r},\mathbf{r}',0)]\cdot\delta\mathbf{A}_s(\mathbf{r}',\omega) + \chi_{s,\mathbf{j}_p\rho}(\mathbf{r},\mathbf{r}',\omega)\delta v_s(\mathbf{r}',\omega)\}d\mathbf{r}'. \tag{10}$$

This provides an efficient way to deal with the incompleteness of the basis set in the $\omega\to 0$ limit in actual applications. In Eq. (10), the Kohn-Sham potentials are, to first order, given by

$$\delta\mathbf{A}_s(\mathbf{r},\omega) = \delta\mathbf{A}_{\mathrm{mac}}(\omega) + \delta\mathbf{A}_{xc}(\mathbf{r},\omega), \tag{11}$$

$$\delta v_s(\mathbf{r},\omega) = \delta v_{H,\mathrm{mic}}(\mathbf{r},\omega) + \delta v_{xc,\mathrm{mic}}(\mathbf{r},\omega), \tag{12}$$

where we chose the gauge such that all components that represent a macroscopic field are included in the vector potential since we choose the scalar potential to be lattice periodic.[35] In Eq. (12), $\delta v_{H,\mathrm{mic}}(\mathbf{r},\omega)$ is the microscopic part of the Hartree potential and $\delta v_{xc,\mathrm{mic}}(\mathbf{r},\omega)$ is the microscopic part of the exchange-correlation scalar potential. The macroscopic vector potential $\delta\mathbf{A}_{\mathrm{mac}}(\omega)$ consists of the external plus the induced vector potential. The latter potential accounts for the long-range contribution of the Hartree potential of the surface charge and for the retarded contribution of the induced transverse current density. We can safely neglect the microscopic part of the induced vector potential because its electric-field contribution is already a factor ω^2/c^2 smaller than that of the microscopic Hartree potential.[35] This is consistent with the Breit approximation used in the ground-state calculation.[36,37] The gauge is chosen such that the external field is incorporated into $\delta\mathbf{A}_{\mathrm{mac}}(\omega)$. Finally, $\delta\mathbf{A}_{xc}(\mathbf{r},\omega)$ is the exchange-correlation vector potential. In practice, an approximation is required for the set of exchange-correlation potentials $\{\delta v_{xc}(\mathbf{r},\omega),\delta\mathbf{A}_{xc}(\mathbf{r},\omega)\}$.

In Sec. II B, we will discuss the expression that Vignale and Kohn derived for $\delta\mathbf{A}_{xc}(\mathbf{r},\omega)$. In this derivation, they chose the gauge such that $\delta v_{xc}(\mathbf{r},\omega)$ vanishes for all frequencies ω. It turns out that a part of their final expression for $\delta\mathbf{A}_{xc}(\mathbf{r},\omega)$ is equal to the gradient of the ALDA exchange-correlation scalar potential. This part can then be gauge transformed into $\delta v_{xc,\mathrm{mic}}(\mathbf{r},\omega)$.

B. Vignale-Kohn functional

The general expression for the exchange-correlation vector potential to first order is

$$\delta A_{xc,i}(\mathbf{r},\omega) = \sum_j \int d\mathbf{r}' f_{xc,ij}(\mathbf{r},\mathbf{r}',\omega)\delta j_j(\mathbf{r}',\omega), \tag{13}$$

which defines the tensor kernel $\overleftrightarrow{f}_{xc}(\mathbf{r},\mathbf{r}',\omega)$. Vignale and Kohn derived an approximation for this exchange-correlation kernel.[11,12] For this, they studied a periodically modulated electron gas with wave vector $\mathbf{q}$, i.e.,

$$\rho_0(\mathbf{r}) = \rho[1+2\gamma\cos(\mathbf{q}\cdot\mathbf{r})], \tag{14}$$

where ρ is the density of the homogeneous electron gas and $\gamma\ll 1$, and performed an expansion of the exchange-correlation kernel

$$f_{xc,ij}(\mathbf{k}+m\mathbf{q},\mathbf{k},\omega) = \frac{1}{\Omega}\int d\mathbf{r}\int d\mathbf{r}' f_{xc,ij}(\mathbf{r},\mathbf{r}',\omega)e^{-i(\mathbf{k}+m\mathbf{q})\cdot\mathbf{r}}e^{i\mathbf{k}\cdot\mathbf{r}'}, \tag{15}$$

to second order in $\mathbf{k}$ and $\mathbf{q}$ and to first order in γ. In Eq. (15),

Ω is the volume of the system and m is an integer for which to first order in γ only the values for $|m| \leq 1$ are needed. This expansion was shown to be analytic for small $\mathbf{k}$ and $\mathbf{q}$ and to be valid under the constraints $k, q \ll k_F, \omega/v_F$, where $k=|\mathbf{k}|$ and $q=|\mathbf{q}|$ and where k_F and v_F are the local Fermi momentum and the Fermi velocity, respectively. The coefficients in this expansion are completely determined in terms of the density ρ and the coefficients $f^h_{xcL}(\rho,\omega)$ and $f^h_{xcT}(\rho,\omega)$ of the exchange-correlation kernel of the homogeneous electron gas by the Onsager symmetry relation, the zero-force and zero-torque theorems and a Ward identity.[11,12] The VK expression for $\delta\mathbf{A}_{xc}(\mathbf{r},\omega)$ is then obtained from

$$\delta A_{xc,i}(\mathbf{r},\omega) = \sum_j \sum_{m=0,\pm 1} \int \frac{d\mathbf{k}}{(2\pi)^3} f_{xc,ij}(\mathbf{k}+m\mathbf{q},\mathbf{k},\omega) \times e^{i(\mathbf{k}+m\mathbf{q})\cdot\mathbf{r}} \delta j_j(\mathbf{k},\omega) \tag{16}$$

by inserting the expansion for $\overleftrightarrow{f}_{xc}$ in Eq. (16) and using Eq. (14). Since this expression contains first- and second-order powers of $\mathbf{k}$, we obtain first- and second-order derivatives of the current density in real space. Similarly first- and second-order powers of $\mathbf{q}$ lead to first- and second-order derivatives of $\rho_0(\mathbf{r})$ in real space. From analysis of Eq. (16) and as a consequence of a Ward identity ρ can be replaced by $\rho_0(\mathbf{r})$ in the coefficients $f^h_{xcL}(\rho,\omega)$ and $f^h_{xcT}(\rho,\omega)$. This will only affect terms of order γ^2, which were already neglected in the derivation. By doing this, we obtain a functional we can apply to general systems, although when applied to systems with large density variations we may go outside the range of validity of the VK derivation. It was shown by Vignale *et al.*[23] and Conti and Vignale[38] that the VK expression for $\delta\mathbf{A}_{xc}(\mathbf{r},\omega)$ could be written in the form of a viscoelastic field

$$i\omega\delta A_{xc,i}(\mathbf{r},\omega) = \partial_i \delta v_{xc}^{\mathrm{ALDA}}(\mathbf{r},\omega) - \frac{1}{\rho_0(\mathbf{r})} \sum_j \partial_j \sigma_{xc,ij}(\mathbf{r},\omega), \tag{17}$$

where $\delta v_{xc}^{\mathrm{ALDA}}(\mathbf{r},\omega)$ is the linearization of the ALDA exchange-correlation scalar potential and $\overleftrightarrow{\sigma}_{xc}(\mathbf{r},\omega)$ is a tensor field, which has the structure of a symmetric viscoelastic stress tensor,

$$\sigma_{xc,ij} = \tilde{\eta}_{xc}\left(\partial_j u_i + \partial_i u_j - \frac{2}{3}\delta_{ij}\sum_k \partial_k u_k\right) + \tilde{\zeta}\delta_{ij}\sum_k \partial_k u_k, \tag{18}$$

in which the velocity field $\mathbf{u}(\mathbf{r},\omega)$ is given by

$$\mathbf{u}(\mathbf{r},\omega) = \frac{\delta\mathbf{j}(\mathbf{r},\omega)}{\rho_0(\mathbf{r})}. \tag{19}$$

The coefficients $\tilde{\eta}_{xc}(\mathbf{r},\omega)$ and $\tilde{\zeta}_{xc}(\mathbf{r},\omega)$ are determined by the longitudinal and transverse response coefficients $f^h_{xcL}[\rho_0(\mathbf{r}),\omega]$ and $f^h_{xcT}[\rho_0(\mathbf{r}),\omega]$ of the homogeneous electron gas evaluated at the density $\rho_0(\mathbf{r})$,

$$\tilde{\eta}_{xc}(\mathbf{r},\omega) = \frac{i}{\omega}\rho_0^2(\mathbf{r}) f^h_{xcT}[\rho_0(\mathbf{r}),\omega], \tag{20}$$

and

$$\tilde{\zeta}_{xc}(\mathbf{r},\omega) = \frac{i}{\omega}\rho_0^2(\mathbf{r})\left(f^h_{xcL}[\rho_0(\mathbf{r}),\omega] - \frac{4}{3}f^h_{xcT}[\rho_0(\mathbf{r}),\omega] - \frac{d^2\epsilon^h_{xc}}{d\rho^2}[\rho_0(\mathbf{r})]\right), \tag{21}$$

where $\epsilon^h_{xc}(\rho)$ is the exchange-correlation energy per unit volume of the homogeneous electron gas. The quantities $\tilde{\eta}_{xc}(\mathbf{r},\omega)$ and $\tilde{\zeta}_{xc}(\mathbf{r},\omega)$ can be interpreted as viscoelastic coefficients.[23,38] The parameter $\tilde{\zeta}_{xc}(\mathbf{r},\omega)$ contains a factor for which one can prove the exact relation[23,38]

$$\lim_{\omega\to 0}\left(f^h_{xcL}[\rho_0(\mathbf{r}),\omega] - \frac{4}{3}f^h_{xcT}[\rho_0(\mathbf{r}),\omega] - \frac{d^2\epsilon^h_{xc}}{d\rho^2}[\rho_0(\mathbf{r})]\right) = 0. \tag{22}$$

As mentioned before, the validity of the expression in Eqs. (17)–(21) has been rigorously proven under the constraints $k, q \ll k_F, \omega/v_F$.[11,12] From Eq. (14), we see that the constraint $q \ll k_F, \omega/v_F$ implies in real space that

$$\frac{|\nabla\rho_0(\mathbf{r})|}{\rho_0(\mathbf{r})} \lesssim 2\gamma q \ll k_F, \frac{\omega}{v_F}. \tag{23}$$

To obtain an expression for the constraint $k \ll k_F, \omega/v_F$ in real space, we start from the expression of the induced current density for the homogeneous electron gas

$$\delta\mathbf{j}(\mathbf{r},\omega) = \int d\mathbf{r}' \chi_{\mathbf{jj}}(\mathbf{r}-\mathbf{r}',\omega)\cdot\delta\mathbf{A}(\mathbf{r}',\omega). \tag{24}$$

It is convenient to do a Fourier transformation with respect to $(\mathbf{r}-\mathbf{r}')$. We obtain

$$\delta\mathbf{j}(\mathbf{r},\omega) = \int \frac{d\mathbf{k}}{(2\pi)^3} e^{i\mathbf{k}\cdot\mathbf{r}} \chi_{\mathbf{jj}}(\mathbf{k},\omega)\cdot\delta\mathbf{A}(\mathbf{k},\omega), \tag{25}$$

where the Fourier transform and its inverse are given by

$$f(\mathbf{k}) = \int d\mathbf{r} e^{-i\mathbf{k}\cdot\mathbf{r}} f(\mathbf{r}) \tag{26}$$

$$f(\mathbf{r}) = \int \frac{d\mathbf{k}}{(2\pi)^3} e^{i\mathbf{k}\cdot\mathbf{r}} f(\mathbf{k}). \tag{27}$$

We can define the longitudinal and transverse parts of $\chi_{\mathbf{jj}}(\mathbf{k},\omega)$ denoted by $\chi_L(\mathbf{k},\omega)$ and $\chi_T(\mathbf{k},\omega)$, respectively, according to

$$\chi_{\mathbf{jj},mn}(\mathbf{k},\omega) = \chi_L(\mathbf{k},\omega)\frac{k_m k_n}{k^2} + \chi_T(\mathbf{k},\omega)\left(\delta_{mn} - \frac{k_m k_n}{k^2}\right). \tag{28}$$

It then follows that we have the following expressions:

$$\nabla\cdot\delta\mathbf{j}(\mathbf{r},\omega) = \int \frac{d\mathbf{k}}{(2\pi)^3} i e^{i\mathbf{k}\cdot\mathbf{r}} \chi_L(\mathbf{k},\omega)\mathbf{k}\cdot\delta\mathbf{A}(\mathbf{k},\omega) \tag{29}$$

$$\nabla \times \delta\mathbf{j}(\mathbf{r},\omega) = \int \frac{d\mathbf{k}}{(2\pi)^3} i e^{i\mathbf{k}\cdot\mathbf{r}} \chi_T(\mathbf{k},\omega)\mathbf{k} \times \delta\mathbf{A}(\mathbf{k},\omega). \tag{30}$$

We now consider a vector potential that is consistent with the slowly varying external perturbation considered in the derivation of the VK functional, i.e., $\delta\mathbf{A}(\mathbf{k},\omega)=\delta(\mathbf{k}-\mathbf{k}_0)[\mathbf{A}_L(\mathbf{k},\omega)+\mathbf{A}_T(\mathbf{k},\omega)]$ with $|\mathbf{k}_0| \ll k_F, \omega/v_F$ and $\mathbf{A}_{L(T)}(\mathbf{k},\omega)$ the longitudinal (transverse) part of the vector potential for which we have $\mathbf{k}\cdot\mathbf{A}_T(\mathbf{k},\omega)=\mathbf{k}\times\mathbf{A}_L(\mathbf{k},\omega)=0$. We then obtain

$$|\nabla \cdot \delta\mathbf{j}(\mathbf{r},\omega)| = |\mathbf{k}_0||\delta\mathbf{j}_L(\mathbf{r},\omega)| \leq |\mathbf{k}_0||\delta\mathbf{j}(\mathbf{r},\omega)| \tag{31}$$

$$|\nabla \times \delta\mathbf{j}(\mathbf{r},\omega)| = |\mathbf{k}_0||\delta\mathbf{j}_T(\mathbf{r},\omega)| \leq |\mathbf{k}_0||\delta\mathbf{j}(\mathbf{r},\omega)|, \tag{32}$$

where the longitudinal (transverse) part of the induced current density $\delta\mathbf{j}_{L(T)}(\mathbf{r},\omega)$ is the inverse Fourier transform of $\delta\mathbf{j}_{L(T)}(\mathbf{k},\omega)=\chi_{L(T)}(\mathbf{k},\omega)\delta\mathbf{A}_{L(T)}(\mathbf{k},\omega)$. We thus see that the condition $k \ll k_F, \omega/v_F$ implies that

$$\frac{|\nabla \cdot \delta\mathbf{j}(\mathbf{r},\omega)|}{|\delta\mathbf{j}(\mathbf{r},\omega)|} \ll k_F, \frac{\omega}{v_F}. \tag{33}$$

$$\frac{|\nabla \times \delta\mathbf{j}(\mathbf{r},\omega)|}{|\delta\mathbf{j}(\mathbf{r},\omega)|} \ll k_F, \frac{\omega}{v_F}. \tag{34}$$

Therefore, Eq. (33) is a measure for the degree in which the longitudinal part of the current density satisfies the constraint $k_L \ll k_F, \omega/v_F$ and Eq. (34) is a measure for the degree in which the transverse part of the current density satisfies the constraint $k_T \ll k_F, \omega/v_F$, where $k_{L(T)}$ is the length of the longitudinal (transverse) part of $\mathbf{k}$.

C. Limiting behavior of $f^h_{xcL,T}$

In the VK functional enter the longitudinal and transverse response kernels of the homogeneous electron gas $f^h_{xcL,T}(\omega)$. These are obtained from $f^h_{xcL,T}(\mathbf{k},\omega)$ in the limit $\mathbf{k}\to 0$. Let us now evaluate these kernels in the limit $\omega \to 0$. From a viscoelastic analysis by Conti and Vignale,[38] we know that we obtain the following relations in that limit:

$$\lim_{\omega\to 0}\lim_{\mathbf{k}\to 0} f^h_{xcL}(\mathbf{k},\omega) = \frac{1}{\rho^2}\left(K_{xc} + \frac{4}{3}\mu_{xc}\right) \tag{35}$$

$$= \frac{d^2\epsilon^h_{xc}(\rho)}{d\rho^2} + \frac{4}{3}\frac{\mu_{xc}}{\rho^2} \tag{36}$$

$$\lim_{\omega\to 0}\lim_{\mathbf{k}\to 0} f^h_{xcT}(\mathbf{k},\omega) = \frac{\mu_{xc}}{\rho^2}, \tag{37}$$

where K_{xc} and μ_{xc} are the exchange-correlation parts of the bulk modulus and shear modulus, respectively. The order of limits in Eqs. (35) and (37) guarantees that the evaluation of $f^h_{xcL,T}(\mathbf{k},\omega)$ in $(\mathbf{k}=0,\omega=0)$ is in the region above the particle-hole continuum. We see that if the limit $\mathbf{k}\to 0$ is taken before the limit $\omega\to 0$ there remains a finite contribution from $f^h_{xcL}(\mathbf{k},\omega)$ as well as $f^h_{xcT}(\mathbf{k},\omega)$. The order in which the limits are taken in Eqs. (35) and (37) is important because, taking the reverse order of limits leads to the following expressions:

$$\lim_{\mathbf{k}\to 0}\lim_{\omega\to 0} f^h_{xcL}(\mathbf{k},\omega) = \frac{d^2\epsilon^h_{xc}(\rho)}{d\rho^2} \tag{38}$$

$$\lim_{\mathbf{k}\to 0}\lim_{\omega\to 0} f^h_{xcT}(\mathbf{k},\omega) = \lim_{\mathbf{k}\to 0}\lim_{\omega\to 0}\frac{\omega^2}{k^2}\left(\frac{1}{\chi_{T,s}(\mathbf{k},\omega)} - \frac{1}{\chi_T(\mathbf{k},\omega)}\right) = 0, \tag{39}$$

where $\chi_{T,s}(\mathbf{k},\omega)$ is the transverse part of the Kohn-Sham current-current response function. The first expression is obtained from the compressibility sum rule.[39] The second expression vanishes because in the limit $\omega\to 0$ both $\chi_{T,s}(\mathbf{k},\omega)$ and $\chi_T(\mathbf{k},\omega)$ have finite values. That $\chi_{T,s}(\mathbf{k},\omega)$ has a finite value in the limit $\omega\to 0$ follows from the evaluation of the Lindhard function in that limit. Furthermore, we know from Landau theory that[14]

$$\lim_{\mathbf{k}\to 0}\chi_T(\mathbf{k},\omega=0) = -\rho, \tag{40}$$

from which it is clear that $\chi_T(\mathbf{k},\omega)$ is finite in the limit $\omega\to 0$. The order of limits in Eqs. (38) and (39) guarantees that the evaluation of $f^h_{xcL,T}(\mathbf{k},\omega)$ in $(\mathbf{k}=0,\omega=0)$ is within the particle-hole continuum. From a comparison of Eqs. (36) and (37) and Eqs. (38) and (39), we see that in the limit $(\mathbf{k},\omega)\to(0,0)$ the exchange-correlation kernels $f^h_{xcL,T}(\mathbf{k},\omega)$ have a discontinuity that is proportional to μ_{xc}. Although the precise value of μ_{xc} is unknown, it is much smaller than K_{xc}. However, it turns out that it has a big influence on the optical spectra of one- and three-dimensional polyacetylene calculated with the VK functional.[32] In fact, surprisingly, the influence on the optical spectra of the terms in the VK functional involving the transverse kernel $f^h_{xcT}(\omega)$ is much bigger than the terms involving the longitudinal kernel $f_{xcL}(\omega)$. These terms are responsible for a large shift of the peak that appears in the optical spectra of one- and three-dimensional polyacetylene to higher frequency with respect to the peak in the ALDA spectra. Furthermore, they cause a large reduction of the height of this peak. However, if one makes the approximation $\mu_{xc}=0$, which effectively is the same as using Eqs. (38) and (39) instead of Eqs. (36) and (37), we obtained results that are close to the results obtained within the ALDA. The reason is that within this approximation the VK functional reduces to the ALDA in the limit $\omega\to 0$, as can be seen from Eqs. (17)–(22), and the fact that the values of $f^h_{xcL,T}(\omega)$ do not change much from their values at $\omega=0$ for $\omega \ll \omega_{pl}$, where ω_{pl} is the plasmon frequency. This is typically the frequency range in which we are interested. From the above considerations, it seems that the VK functional gives too much weight to the transverse kernel $f_{xcT}(\omega)$ when it is applied to the calculation of the optical spectra of systems with inhomogeneous ground-state densities. Furthermore, since the optical spectrum of a system is closely related to its particle-hole continuum and, in view of the discontinuity of $f_{xcL,T}(\mathbf{k},\omega)$ in $(0,0)$, it might be more desirable to employ a

functional in which the kernels $f^h_{xcL,T}(\mathbf{k},\omega)$ are evaluated in the particle-hole continuum instead of in the region above the particle-hole continuum. However, one should consider a finite $\mathbf{k}$ throughout the derivation of such a functional since taking the limit $\mathbf{k}\to 0$ at any stage in the derivation has the consequence that $f^h_{xcL,T}(\mathbf{k},\omega)$ have to be evaluated in the region above the particle-hole continuum. The exception to the above statement is when the limit $\omega\to 0$ is taken before the limit $\mathbf{k}\to 0$, as is effectively done to obtain the ALDA, for example.

D. Parametrizations for $f^h_{xcL,T}$

In a previous paper, we discussed extensively the parametrizations that are available for $f^h_{xcL,T}[\rho_0(\mathbf{r}),\omega]$.[32] Here, we will give a brief summary. Gross and Kohn (GK) obtained exact properties of $f^h_{xcL}(\mathbf{k}=0,\omega)\equiv f^h_{xcL}(\omega)$ in the low- and high-frequency limits.[40,41] Furthermore, they introduced an interpolation formula for $\mathrm{Im}\, f^h_{xcL}(\omega)$ that reduces to the exact high-frequency limit for $\omega\to\infty$ obtained from second-order perturbative expansions by Glick and Long[42] and vanishes linearly in the limit $\omega\to 0$. The real part of $f^h_{xcL}(\omega)$ can subsequently be obtained from the Kramers-Krönig dispersion relations. However, in deriving this interpolation formula they implicitly made the assumption that $\lim_{\omega\to 0}\lim_{\mathbf{k}\to 0} f^h_{xcL}(\mathbf{k},\omega)=\lim_{\mathbf{k}\to 0}\lim_{\omega\to 0} f^h_{xcL}(\mathbf{k},\omega)=d^2\epsilon^h_{xc}(\rho)/d\rho^2$ which from Sec. II C we know to be wrong. A different approach to obtain $f^h_{xcL}(\omega)$ as well as $f^h_{xcT}(\omega)$ was given by Conti, Nifosì, and Tosi (CNT).[43] They calculated $\mathrm{Im}\, f^h_{xcL,T}(\omega)$ by direct evaluation of the imaginary parts of the longitudinal and transverse parts of the current-current response functions, $\mathrm{Im}\,\chi_{L,T}(\mathbf{k},\omega)$. CNT used exact expressions for $\mathrm{Im}\,\chi_{L,T}(\mathbf{k},\omega)$ in terms of four-point response functions that were subsequently approximated by decoupling them into products of two-point response functions. In order to include the effect of plasmons, the two-point response functions were then taken to be the response functions in the random-phase approximation (RPA). This decoupling scheme only keeps direct contributions and neglects exchange processes. To account for the latter processes, CNT introduced a phenomenological factor that reduces the total two-pair spectral weight by a factor of 2 in the high-frequency limit. In the low-frequency limit, the factor is close to unity for metallic densities, thereby largely neglecting exchange processes. A distinct feature of the CNT result is a pronounced peak at $\omega=2\omega_{pl}$ in $\mathrm{Im}\, f^h_{xcL,T}(\omega)$. The high-frequency behavior of $\mathrm{Im}\, f^h_{xcL}(\omega)$ obtained by CNT coincides with the result of Glick and Long,[42] and the high-frequency behavior of $\mathrm{Im}\, f^h_{xcT}(\omega)$ given by CNT is new. Furthermore, CNT introduced parametrizations for $\mathrm{Im}\, f^h_{xcL,T}(\omega)$ that reproduce their numerical results. The real parts can again be obtained from the Kramers-Krönig dispersion relations, where the high-frequency limits of $f^h_{xcL,T}(\omega)$ were obtained from third-frequency-moment sum rules.[38,39,41] Like GK, CNT neglect the discontinuity of $f_{xcL,T}(\mathbf{k},\omega)$ in $(\mathbf{k},\omega)=(0,0)$ because they prefer to enforce continuity in the limit $(\mathbf{k},\omega)\to(0,0)$ since they expect the discontinuity in this limit to be small and since the exact value of this discontinuity is unknown. Neglecting this discontinuity effectively amounts to the approximation $\mu_{xc}=0$.

Qian and Vignale (QV)[44] combined the methods of GK and CNT. They obtained an analytic result for the slope of $\mathrm{Im}\, f^h_{xcT}(\omega)$ at $\omega=0$ by evaluating $\mathrm{Im}\,\chi_{L,T}(\mathbf{k},\omega)$ within perturbation theory in a similar way as CNT. The direct contributions were treated the same, but QV also included their exchange counterparts in the evaluation. They adopted the interpolation scheme of GK for $\mathrm{Im}\, f^h_{xcT}(\omega)$ in which they need one more parameter to satisfy the new constraint on the slope of $\mathrm{Im}\, f^h_{xcL,T}(\omega)$ at $\omega=0$. This extra parameter in their scheme is the width of a Gaussian peak around $\omega=2\omega_{pl}$ that accounts for the two-plasmon contributions found by CNT. The coefficients in their interpolation formula are now determined by their analytic result for the slope at $\omega=0$ and the correct low-frequency limits, Eqs. (36) and (37), as well as the correct high-frequency behavior. The values for μ_{xc} were obtained from the Landau parameters calculated by Yasuhara and Ousaka[45] for some values of the Wigner-Seitz radius r_s $(4\pi r_s^3/3=1/\rho)$. Their model shows a peak around $\omega=2\omega_{pl}$ that is less pronounced than CNT's.

Since the CNT parametrization for $f^h_{xcL,T}(\omega)$ is based on the approximation $\mu_{xc}=0$, the VK functional with this parametrization reduces to the ALDA in the limit $\omega\to 0$. The static limit of the VK functional with the QV parametrization for $f^h_{xcL,T}(\omega)$ is not equal to the ALDA since in this parametrization $f^h_{xcT}(0)$ is nonzero. The approximation $\mu_{xc}=0$ can easily be included in the QV interpolation formula and we will denote this approximated form of the QV parametrization for $f^h_{xcL,T}(\omega)$ by QVA.

III. COMPUTATIONAL DETAILS

The implementation was done in the ADF-BAND program,[35,46–48] and we performed our calculations with this modified version. We made use of Slater-type orbitals (STO) in combination with frozen cores and a hybrid valence basis set consisting of the numerical solutions of a free-atom Herman-Skillman program[49] that solves the radial Kohn-Sham equations. The spatial resolution of this basis is equivalent to a STO triple-ζ basis set augmented with two polarization functions. This valence basis set was made orthogonal to the core states. The Herman-Skillman program also provides us with the free-atom effective potential. The Hartree potential was evaluated using an auxiliary basis set of STO functions to fit the deformation density in the ground-state calculation and the induced density in the response calculation. We used the VK functional to calculate the dielectric function of silicon. We used Eqs. (1) and (2) to obtain $\chi_e(\omega)$ from which the macroscopic dielectric function can directly be obtained through $\epsilon(\omega)=\epsilon_1(\omega)+i\epsilon_2(\omega)=1+4\pi\chi_e(\omega)$. For the evaluation of the $\mathbf{k}$-space integrals, we used a numerical integration scheme with 369 symmetry-unique sample points in the irreducible wedge of the Brillouin zone, which was constructed by adopting a Lehmann-Taut tetrahedron scheme.[50] We checked the convergence with respect to the number of conduction bands used and found that ten conduction bands are sufficient. This number

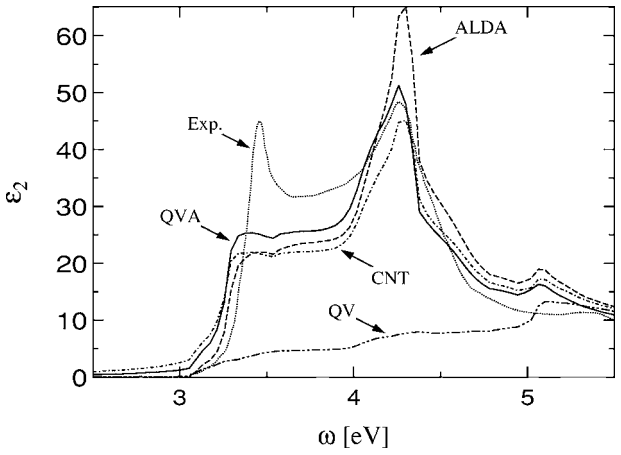

FIG. 1. The calculated and measured imaginary part of the dielectric function $[\epsilon_2(\omega)]$ of silicon. The calculated spectra were obtained using the ALDA as well as the VK functional with the QV, QVA, and CNT parametrizations for the exchange-correlation kernels of the homogeneous electron gas. The experimental result is taken from Ref. 52. Dashed curve: ALDA; dotted dashed curve: VK with CNT; double dotted dashed curve: VK with QV; continuous curve: VK with QVA; dotted curve: experiment.

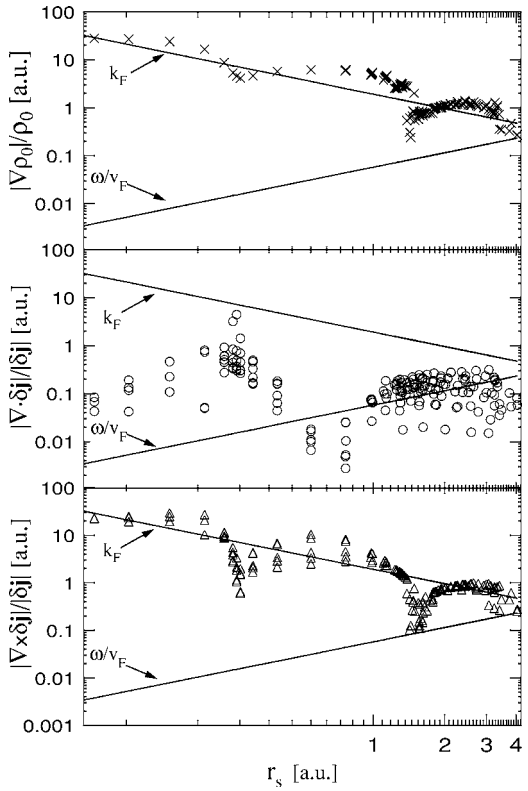

FIG. 2. Test of the constraints (23), (33), and (34) at $\omega=3$ eV for silicon. The results were obtained using the VK functional with the QV parametrization for the longitudinal and transverse exchange-correlation kernels of the homogeneous electron gas. In the graph, $r_s(\mathbf{r})$ is the local Wigner-Seitz radius $[4\pi r_s^3(\mathbf{r})/3 = 1/\rho_0(\mathbf{r})]$. All quantities were calculated on the spatial grid that was used in the calculations. The top line in each panel: k_F; bottom line in each panel: ω/v_F; crosses: $|\nabla\rho_0(\mathbf{r})|/\rho_0(\mathbf{r})$; circles: $|\nabla\cdot\delta\mathbf{j}(\mathbf{r},\omega)|/|\delta\mathbf{j}(\mathbf{r},\omega)|$; triangles: $|\nabla\times\delta\mathbf{j}(\mathbf{r},\omega)|/|\delta\mathbf{j}(\mathbf{r},\omega)|$.

was used in all our calculations. We made use of the Vosko-Wilk-Nusair parametrization[51] of the LDA exchange-correlation potential, which was also used to construct the ALDA exchange-correlation kernel. As mentioned above, the values for $f^h_{xcL,T}(\rho,\omega)$ were obtained from the parametrizations given in Refs. 43 and 44 denoted by CNT and QV, respectively. In the QV interpolation formula for $\mathrm{Im}\, f^h_{xcT}(\rho,\omega)$, we need $f^h_{xcT}(\rho,0)$. This quantity is known only at specific values of the Wigner-Seitz radius r_s. We used a cubic spline interpolation to obtain values for $f^h_{xcT}(\rho,0)$ at arbitrary r_s in which the behavior for small r_s was taken to be quadratic similar to exchange-only behavior.

IV. RESULTS

As a typical example for the optical spectra obtained with TDCDFT using the VK functional, we report the imaginary part of dielectric function of silicon in Fig. 1. We also performed calculations on several other semiconductors and insulators, namely, GaAs, GaP, and diamond and found qualitatively similar results. The various results in Fig. 1 correspond to different approximations for $f^h_{xcL,T}(\rho,\omega)$ that enter the VK expression for $\delta\mathbf{A}_{xc}(\mathbf{r},\omega)$. We compare our results obtained with the VK functional to our ALDA results and with results obtained from experiment.[52] In order to facilitate comparison, we have used a scissors operator in our calculations to coincide the calculated optical gap with that found in experiment. The scissors operator shifts upward the energies of the unoccupied Kohn-Sham orbitals and changes the matrix elements of the current operator. The spectrum obtained with the QV interpolation formula for $f^h_{xcL,T}(\rho,\omega)$ collapses. The spectra obtained with the CNT and QVA parametrizations, however, are close to the ALDA spectrum. They even show some improvement over the ALDA spectrum because the height of the second peak is better reproduced. As mentioned before the CNT and QVA spectra are close to the ALDA spectrum because the VK functional with the CNT or QVA parametrization for $f^h_{xcL,T}(\rho,\omega)$ reduces to the ALDA in the limit $\omega\to 0$ and the fact that the values of $f^h_{xcL,T}(\omega)$ in these parametrizations do not change much from their values at $\omega=0$ for $\omega\ll\omega_{pl}$, which is typically the frequency range that we are interested in. From a comparison between the QV and QVA spectra, we can conclude that the transverse kernel $f^h_{xcT}(\rho,\omega)$ has a large unwanted effect on the shape of the spectrum. Since $f^h_{xcT}(\rho,\omega)$ is much smaller than $f^h_{xcL}(\rho,\omega)$ for $\omega\ll\omega_{pl}$ but has a much larger effect on the shape of the spectra, $f^h_{xcT}(\rho,\omega)$ must couple with terms in the VK functional that become large for systems with densities and current densities that are not slowly varying.

Finally, to give an impression of the degree that the constraints (23), (33), and (34) are violated when the Vignale-Kohn functional is applied to the calculation of optical absorption spectra of real systems, we show in Fig. 2 the results we obtain for silicon at $\omega=3$ eV using the QV parametrization. Note the logarithmic scale that is used. All the quantities were calculated on the spatial grid that was used in the calculations. We have tested the dependence of the results on

the frequency and found that this dependence is small for the frequency range in which we are interested. The results also do not depend much on the parametrization that is used. We can roughly make the following conclusions based on Fig. 2,

$$\frac{|\nabla\rho_0(\mathbf{r})|}{\rho_0(\mathbf{r})} \simeq \frac{|\nabla\times\delta\mathbf{j}(\mathbf{r},\omega)|}{|\delta\mathbf{j}(\mathbf{r},\omega)|} \gtrsim k_F \gg \frac{\omega}{v_F} \tag{41}$$

$$k_F \gg \frac{|\nabla\cdot\delta\mathbf{j}(\mathbf{r},\omega)|}{|\delta\mathbf{j}(\mathbf{r},\omega)|} \gtrsim \frac{\omega}{v_F}. \tag{42}$$

We observe that all the constraints except one are violated, and in particular, the constraints $k,q \ll \omega/v_F$. From these considerations, it is therefore not surprising that the results we obtain for the optical spectra of silicon and other materials are not in agreement with experiment.

V. CONCLUSIONS

In this work, we applied the Vignale-Kohn current functional to the calculation of the optical spectra of semiconductors. We discussed our results for silicon. Qualitatively similar results were obtained for other semiconductors. We showed that the optical spectrum collapses when we use the QV parametrization for the longitudinal and transverse exchange-correlation kernels $f^h_{xcL,T}(\omega)=\lim_{\mathbf{k}\to 0} f^h_{xcL,T}(\mathbf{k},\omega)$. We discussed possible reasons for this failure. We showed that the constraints on the degree of nonuniformity of the ground-state density, i.e., $q \ll k_F, \omega/v_F$, and on the degree of the spatial variation of the external potential, i.e., $k \ll k_F, \omega/v_F$, under which the Vignale-Kohn functional was derived are almost all violated. Furthermore, since the Vignale-Kohn functional was derived for a weakly inhomogeneous electron gas in the region above the particle-hole continuum, we argue that it might not be suited to use in the calculation of optical spectra which are closely related to the particle-hole continuum, especially because the longitudinal and transverse exchange-correlation kernels $f^h_{xcL,T}(\mathbf{k},\omega)$ have a discontinuity in $(\mathbf{k}=0,\omega=0)$. We showed that when we use the CNT or QVA parametrizations for $f^h_{xcL,T}(\omega)$, in which the approximation is used that $f^h_{xcL,T}(\mathbf{k},\omega)$ is continuous in $(\mathbf{k}=0,\omega=0)$, which is equivalent to the approximation $\mu_{xc}=0$, the optical spectrum is close to that obtained within the ALDA. This is a consequence of the fact that in this approximation the Vignale-Kohn functional reduces to the ALDA in the limit $\omega\to 0$ and the fact that the values of the coefficients $f^h_{xcL,T}(\omega)$ are close to the values of $f^h_{xcL,T}(0)$ for $\omega \ll \omega_{pl}$ and should not be explained as if the CNT and QVA parametrizations are more accurate than the QV parametrization. The constraints $k,q \ll k_F, \omega/v_F$ are as much violated for the CNT and QVA parametrizations as for the QV parametrization. The results might improve if one or both of these constraints in the VK theory can be relieved to some extent, for example, by avoiding the approximation that the ground-state density is slowly varying.[53]

[1] E. Runge and E. K. U. Gross, Phys. Rev. Lett. **52**, 997 (1984).
[2] E. K. U. Gross and W. Kohn, Adv. Quantum Chem. **21**, 255 (1990).
[3] E. K. U. Gross, J. F. Dobson, and M. Petersilka, Top. Curr. Chem. **181**, 81 (1996).
[4] R. van Leeuwen, Int. J. Mod. Phys. B **15**, 1969 (2001).
[5] A. K. Dhara and S. K. Ghosh, Phys. Rev. A **35**, 442 (1987).
[6] S. K. Ghosh and A. K. Dhara, Phys. Rev. A **38**, 1149 (1988).
[7] G. Vignale, Phys. Rev. B **70**, 201102(R) (2004).
[8] G. D. Mahan and K. R. Subbaswami, *Local Density Theory of Polarizability* (Plenum Press, New York, 1990).
[9] G. Onida, L. Reining, and A. Rubio, Rev. Mod. Phys. **74**, 601 (2002).
[10] O.-J. Wacker, R. Kümmel, and E. K. U. Gross, Phys. Rev. Lett. **73**, 2915 (1994).
[11] G. Vignale and W. Kohn, Phys. Rev. Lett. **77**, 2037 (1996).
[12] G. Vignale and W. Kohn, in *Electronic Density Functional Theory: Recent Progress and New Directions*, edited by J. Dobson, M. P. Das, and G. Vignale (Plenum Press, New York, 1998).
[13] X. Gonze, P. Ghosez, and R. W. Godby, Phys. Rev. Lett. **74**, 4035 (1995); **78**, 294 (1997).
[14] P. Nozières and D. Pines, *The Theory of Quantum Liquids* (Perseus Books, Cambridge, MA, 1999).
[15] Y.-H. Kim and A. Görling, Phys. Rev. B **66**, 035114 (2002); Phys. Rev. Lett. **89**, 096402 (2002).
[16] R. van Leeuwen, in *Progress in Nonequilibrium Green's Functions II*, edited by M. Bonitz and D. Semkat (World Scientific, Singapore, 2003), pp. 427–435.
[17] F. Sottile, V. Olevano, and L. Reining, Phys. Rev. Lett. **91**, 056402 (2003).
[18] G. Adragna, R. DelSole, and A. Marini, Phys. Rev. B **68**, 165108 (2003).
[19] M. van Faassen, P. L. de Boeij, R. van Leeuwen, J. A. Berger, and J. G. Snijders, Phys. Rev. Lett. **88**, 186401 (2002).
[20] M. van Faassen, P. L. de Boeij, R. van Leeuwen, J. A. Berger, and J. G. Snijders, J. Chem. Phys. **118**, 1044 (2003).
[21] M. van Faassen and P. L. de Boeij, J. Chem. Phys. **121**, 10707 (2004).
[22] S. J. A. van Gisbergen, P. R. T. Schipper, O. V. Gritsenko, E. J. Baerends, J. G. Snijders, B. Champagne, and B. Kirtman, Phys. Rev. Lett. **83**, 694 (1999).
[23] G. Vignale, C. A. Ullrich, and S. Conti, Phys. Rev. Lett. **79**, 4878 (1997).
[24] C. A. Ullrich and G. Vignale, Phys. Rev. B **58**, 7141 (1998).
[25] C. A. Ullrich and G. Vignale, Phys. Rev. B **58**, 15756 (1998).
[26] C. A. Ullrich and G. Vignale, Phys. Rev. Lett. **87**, 037402 (2001).
[27] C. A. Ullrich and G. Vignale, Phys. Rev. B **65**, 245102 (2002).
[28] P. L. de Boeij, F. Kootstra, J. A. Berger, R. van Leeuwen, and J. G. Snijders, J. Chem. Phys. **115**, 1995 (2001).
[29] M. van Faassen and P. L. de Boeij, J. Chem. Phys. **120**, 8353 (2004).
[30] C. A. Ullrich and K. Burke, J. Chem. Phys. **121**, 28 (2004).
[31] M. van Faassen, Int. J. Mod. Phys. B **20**, 3419 (2006).
[32] J. A. Berger, P. L. de Boeij, and R. van Leeuwen, Phys. Rev. B

71, 155104 (2005).
[33] P. Puschnig and C. Ambrosch-Draxl, Phys. Rev. Lett. **89**, 056405 (2002); Synthesis **135-136**, 415 (2003).
[34] M. L. Tiago, M. Rohlfing, and S. G. Louie, Phys. Rev. B **70**, 193204 (2004).
[35] F. Kootstra, P. L. de Boeij, and J. G. Snijders, J. Chem. Phys. **112**, 6517 (2000).
[36] G. Breit, Phys. Rev. **34**, 553 (1929); **39**, 616 (1932).
[37] O. L. Brill and B. Goodman, Am. J. Phys. **35**, 832 (1967).
[38] S. Conti and G. Vignale, Phys. Rev. B **60**, 7966 (1999).
[39] S. Ichimaru, Rev. Mod. Phys. **54**, 1017 (1982).
[40] E. K. U. Gross and W. Kohn, Phys. Rev. Lett. **55**, 2850 (1985); **57**, 923(E) (1986).
[41] N. Iwamoto and E. K. U. Gross, Phys. Rev. B **35**, 3003 (1987).
[42] A. J. Glick and W. F. Long, Phys. Rev. B **4**, 3455 (1971).
[43] S. Conti, R. Nifosí, and M. P. Tosi, J. Phys.: Condens. Matter **9**, L475 (1997).
[44] Z. Qian and G. Vignale, Phys. Rev. B **65**, 235121 (2002).
[45] H. Yasuhara and Y. Ousaka, Int. J. Mod. Phys. B **6**, 3089 (1992).
[46] G. te Velde and E. J. Baerends, Phys. Rev. B **44**, 7888 (1991); J. Comput. Phys. **99**, 84 (1992).
[47] C. Fonseca Guerra, O. Visser, J. G. Snijders, G. te Velde, and E. J. Baerends, in *Methods and Techniques in Computational Chemistry*, edited by E. Clementi and G. Corongiu (STEF, Cagliari, 1995), p. 305.
[48] G. te Velde, F. M. Bickelhaupt, E. J. Baerends, C. Fonseca Guerra, S. J. A. van Gisbergen, J. G. Snijders, and T. Ziegler, J. Comput. Chem. **22**, 931 (2001).
[49] F. Herman and S. Skillman, *Atomic Structure Calculations* (Prentice-Hall, Englewood Cliffs, NJ, 1963).
[50] G. Lehmann and M. Taut, Phys. Status Solidi B **54**, 469 (1972).
[51] S. H. Vosko, L. Wilk, and M. Nusair, Can. J. Phys. **58**, 1200 (1980).
[52] P. Lautenschlager, M. Garriga, L. Viña, and M. Cardona, Phys. Rev. B **36**, 4821 (1987).
[53] J. Tao and G. Vignale, Phys. Rev. Lett. **97**, 036403 (2006).